BIOCHEMISTRY
including biophysical chemistry & molecular biology

Article

pubs.acs.org/biochemistry

A Rhodanine Derivative CCR-11 Inhibits Bacterial Proliferation by Inhibiting the Assembly and GTPase Activity of FtsZ

Parminder Singh,[†] Bhavya Jindal,[†] Avadhesha Surolia,*[,‡] and Dulal Panda*[,†]

[†]Department of Biosciences and Bioengineering, Indian Institute of Technology Bombay, Mumbai 400076, India
[‡]Molecular Biophysics Unit, Indian Institute of Science, Bangalore 560012, India

Supporting Information

ABSTRACT: A perturbation of FtsZ assembly dynamics has been shown to inhibit bacterial cytokinesis. In this study, the antibacterial activity of 151 rhodanine compounds was assayed using *Bacillus subtilis* cells. Of 151 compounds, eight strongly inhibited bacterial proliferation at 2 μM. Subsequently, we used the elongation of *B. subtilis* cells as a secondary screen to identify potential FtsZ-targeted antibacterial agents. We found that three compounds significantly increased bacterial cell length. One of the three compounds, namely, CCR-11 [(*E*)-2-thioxo-5-({[3-(trifluoromethyl)phenyl]furan-2-yl}methylene)thiazolidin-4-one], inhibited the assembly and GTPase activity of FtsZ in vitro. CCR-11 bound to FtsZ with a dissociation constant of 1.5 ± 0.3 μM. A docking analysis indicated that CCR-11 may bind to FtsZ in a cavity adjacent to the T7 loop and that short halogen−oxygen, H-bonding, and hydrophobic interactions might be important for the binding of CCR-11 with FtsZ. CCR-11 inhibited the proliferation of *B. subtilis* cells with a half-maximal inhibitory concentration (IC_{50}) of 1.2 ± 0.2 μM and a minimal inhibitory concentration of 3 μM. It also potently inhibited proliferation of *Mycobacterium smegmatis* cells. Further, CCR-11 perturbed Z-ring formation in *B. subtilis* cells; however, it neither visibly affected nucleoid segregation nor altered the membrane integrity of the cells. CCR-11 inhibited HeLa cell proliferation with an IC_{50} value of 18.1 ± 0.2 μM (~15 × IC_{50} of *B. subtilis* cell proliferation). The results suggested that CCR-11 inhibits bacterial cytokinesis by inhibiting FtsZ assembly, and it can be used as a lead molecule to develop FtsZ-targeted antibacterial agents.

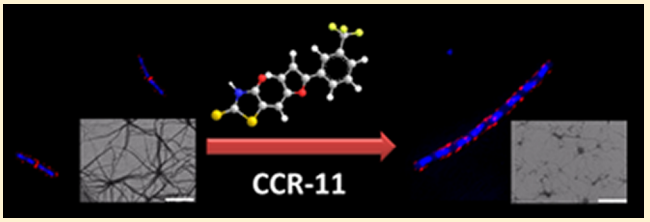

Bacterial cell division machinery involves an array of proteins working in concert leading to a proper cell division. The core protein of the bacterial cell division machinery is FtsZ. Mutations in FtsZ were found to induce cell elongation and to inhibit cell division in *Escherichia coli* at nonpermissive temperatures.[1,2] FtsZ, a GTPase, assembles into protofilaments in a GTP-dependent manner and facilitates cell division with the help of other accessory cell division proteins by forming a contractile ring, called the Z-ring, at the midcell.[3] The Z-ring constricts dividing bacteria into two daughter cells. The Z-ring is a highly dynamic structure, the exchange of GTP-bound FtsZ from the cytosol to the ring and GDP-bound FtsZ from the ring to the cytosol occurring in a continuous manner.[4,5] A perturbation in the dynamics of the Z-ring or its assembly can lead to the impairment of its function, leading to the inhibition of cell division.[3,6−10] Mutations in FtsZ that either inhibit or promote FtsZ assembly have been reported to perturb cytokinesis and cause elongation of bacterial cells.[9,10]

Because of its essential role in cell division, FtsZ is being recognized and investigated as an important antibacterial drug target.[8,11−15] Various synthetic and natural agents that inhibit bacterial cell proliferation by targeting FtsZ have been identified.[13−21] Sanguinarine, a benzophenanthridine alkaloid obtained from the rhizomes of *Sanguinaria canadensis*, was reported to inhibit FtsZ and block cytokinesis in both Gram-positive and Gram-negative bacteria, leading to formation of filamentous cells.[14] Further, totarol, a diterpenoid phenol, has also been reported to target FtsZ assembly, causing inhibition of growth and elongation of *Bacillus subtilis* cells.[16] Many synthetic compounds like zantrins, PC190723, A-189, and 2-carbamoyl pteridine have also been shown to inhibit the growth of bacterial cells by targeting FtsZ.[17−20] Rhodanine series of compounds have been reported to have antibacterial activities.[15,22] For example, OTBA, 3-{5-[4-oxo-2-thioxo-3-(3-trifluoromethylphenyl)thiazolidin-5-ylidenemethyl]furan-2-yl}-benzoic acid, a rhodanine compound, has been found to exhibit antibacterial activity by enhancing the assembly and bundling of FtsZ protofilaments.[15] It stabilized the FtsZ polymers and decreased the GTPase activity of FtsZ.[15]

In this study, we screened a new library (151 compounds) of rhodanine compounds (Chembridge Corp., San Diego, CA) against bacterial proliferation, and eight of these compounds were found to inhibit the proliferation of *B. subtilis* cells by ≥50% at a concentration of 2 μM compared to the control. Several studies suggested that the increase in cell length is a characteristic phenotype associated with the action of FtsZ-

Received: December 9, 2011
Revised: June 16, 2012
Published: June 18, 2012

dx.doi.org/10.1021/bi201813u | *Biochemistry* 2012, 51, 5434−5442

targeted antibacterial agents.[14−16,18,21] Therefore, using cell elongation as a secondary screen, we identified three compounds that might inhibit bacterial cytokinesis by targeting FtsZ. One of the three compounds, CCR-11, was found to inhibit the GTPase activity of purified FtsZ. The data obtained in this study indicate that CCR-11 inhibits bacterial proliferation by targeting FtsZ assembly and suggest that CCR-11 may serve as a lead molecule for the development of FtsZ-targeted antibacterial agents.

MATERIALS AND METHODS

Materials. Piperazine-1,4-bis(2-ethanesulfonic acid) (Pipes), phenylmethanesulfonyl fluoride (PMSF), bovine serum albumin (BSA), β-mercaptoethanol (β-ME), and guanosine 5′-triphosphate (GTP) were purchased from Sigma. FM4−64FX, DAPI, and SYTO9 were purchased from Molecular Probes. Isopropyl β-D-1-thiogalactopyranoside (IPTG) was purchased from Calbiochem. Ni-NTA agarose was purchased from Qiagen. Bio-Gel P6 (medium) was obtained from Bio-Rad. All other chemicals used were of analytical grade. The chemical library was purchased from Chembridge Corp.

Screening of Compounds against Bacterial Cell Proliferation. *B. subtilis* 168 cells were grown to an initial OD_{600} of 0.1. The cells were further grown in the absence and presence of 151 different rhodanine compounds (2 μM each) at 37 °C for 4 h. The growth of bacterial culture was assessed by subtracting the initial OD_{600} from the final OD_{600}. The percentage inhibition of growth in the presence of each compound was calculated with respect to the control. Compounds that were found to inhibit growth by ≥50% at 2 μM were selected, and the morphology of the cells treated with these compounds was examined under a differential interference contrast (DIC) microscope (Nikon ECLIPSE TE2000-U).

Purification of *B. subtilis* FtsZ. *E. coli* BL21(DE3) pLysS cells transformed with the pET16b vector carrying *B. subtilis ftsZ* were grown at 37 °C in Luria-Bertani (LB) medium in the presence of 12.5 μg/mL chloramphenicol and 100 μg/mL ampicillin.[15]The cells were then induced at late log phase (OD_{600} = 0.8) with 1 mM IPTG for 6 h. The cells were harvested and washed with lysis buffer [50 mM NaH_2PO_4 (pH 8.0) and 300 mM NaCl]. The cell pellet was suspended in ice-cold lysis buffer containing 0.1% β-ME and 2 mM PMSF, and 1 mg/mL lysozyme was added and the mixture incubated for 1 h on ice. The cells were then disrupted by sonication (10 pulses for 30 s each), and the crude lysate obtained was clarified by centrifugation at 80000*g* and 4 °C. Then, 5 mM imidazole was added to the cleared cell lysate to prevent nonspecific binding of the proteins to the Ni-NTA resin. The supernatant was then mixed with Ni-NTA resin pre-equilibrated with the lysis buffer containing 5 mM imidazole and incubated with gentle shaking for 1 h at 4 °C. This resin was then loaded on the column, and the flow-through was collected. The column was extensively washed with wash buffer [25 mM Pipes (pH 6.8), 300 mM NaCl, and 75 mM imidazole]. The protein was then eluted with elution buffer [25 mM Pipes (pH 6.8), 300 mM NaCl, and 250 mM imidazole]. FtsZ was then desalted using the Biogel P-6 resin pre-equilibrated with 25 mM Pipes and 50 mM KCl (pH 6.8) and then concentrated using an Amicon 30 kDa centrifugal filter (Millipore). The concentration of FtsZ was determined by the Bradford method[23] using BSA as a standard. The FtsZ concentration was adjusted by including the correction factor of 1.2 for the FtsZ/BSA ratio.[24] FtsZ was stored at −80 °C.

Determination of the GTPase Activity of FtsZ. FtsZ (8 μM) in 25 mM Pipes (pH 6.8) and 50 mM KCl was incubated in the absence and presence of 5, 10, 15, and 20 μM CCR-11 for 10 min on ice. FtsZ was polymerized in the presence of 5 mM $MgCl_2$ and 1 mM GTP at 37 °C for 10 min. The reaction was quenched by adding 10% perchloric acid. The moles of inorganic phosphate released per mole of FtsZ were calculated using the ammonium molybdate assay.[15,25] Similarly, the effect of 5, 10, 15, and 20 μM CCR-4 and CCR-85 on the GTPase activity of FtsZ was also determined.

The effect of 5 and 10 μM CCR-11 on the rate of GTP hydrolysis of FtsZ was estimated. Briefly, FtsZ (8 μM) in 25 mM Pipes (pH 6.8) and 50 mM KCl was incubated in the absence and presence of 5 and 10 μM CCR-11 for 10 min on ice. FtsZ was polymerized in the presence of 5 mM $MgCl_2$ and 1 mM GTP at 37 °C, and the reactions were quenched after 1, 3, 5, 7, and 10 min via the addition of 10% perchloric acid. The moles of inorganic phosphate released per mole of FtsZ were determined using the ammonium molybdate assay, and the rate of hydrolysis was calculated in the absence and presence of 5 and 10 μM CCR-11.

Effects of CCR-11 on the Assembly of FtsZ. *Light Scattering.* FtsZ (8 μM) in 25 mM Pipes (pH 6.8) and 50 mM KCl was incubated without and with 5, 10, and 20 μM CCR-11 on ice for 10 min and then polymerized in the presence of 5 mM $MgCl_2$ and 1 mM GTP. The light scattering at 500 nm was monitored for 300 s at 37 °C using a fluorescence spectrometer (JASCO FP6500).

Electron Microscopy. FtsZ (6 μM) in 25 mM Pipes (pH 6.8) and 50 mM KCl was incubated without and with 5 and 20 μM CCR-11 for 10 min on ice. FtsZ was polymerized in the presence of 5 mM $MgCl_2$ and 1 mM GTP at 37 °C for 5 min. The polymeric suspension was added on a Formvar carbon-coated copper grid (300 mesh), stained with freshly prepared 2% uranyl acetate, and observed using a transmission electron microscope (FEI TECHNAI G^2 12). To rule out the effect of the His tag on the assembly properties of *Bacillus* FtsZ, we removed the His tag from FtsZ using the factor Xa cleavage capture kit (Novagen, EMD chemicals, San Diego, CA) and determined the effects of CCR-11 on the assembly of FtsZ by light scattering and electron microscopy as described above.

Site-Directed Mutagenesis of *B. subtilis* FtsZ. A mutant, Y273W-FtsZ, was constructed by site-directed mutagenesis. The mutated protein was expressed in *E. coli* (BL21) pLysS cells and purified using a protocol similar to that used for wild-type FtsZ.

Determination of the Constant for Binding of CCR-11 to FtsZ. Y273W-FtsZ was found to display assembly kinetics similar to that of wild-type FtsZ. The interaction between CCR-11 and FtsZ was monitored using Y273W-FtsZ. FtsZ in 25 mM Pipes and 50 mM KCl (pH 6.8) was incubated without and with different concentrations (0.25−7 μM) of CCR-11 for 15 min on ice. The tryptophan emission spectra were recorded using an excitation wavelength of 295 nm. The observed fluorescence intensities (at 330 nm) were corrected for inner filter effects using the equation

$$F_{\text{corrected}} = F_{\text{observed}} \times \text{antilog}\,\frac{OD_{\text{excitation}}+OD_{\text{emission}}}{2}$$

The change in the fluorescence of FtsZ in the presence of the compound with respect to control was fit to the equation ΔF =

$(\Delta F_{max}L)/(K_d + L)$ using GraphPad Prism 5, and the dissociation constant was determined. The experiment was repeated three times.

Docking Methodology. To identify the putative binding site of CCR-11 on *B. subtilis* FtsZ, molecular docking was performed using Autodock 4.[26] The structure of *Bacillus* FtsZ was obtained from Protein Data Bank (PDB) entry 2VXY,[27] and the CCR-11 topology was obtained from the PRODRG server.[28] The entire FtsZ molecule was enclosed in a grid box of 170 Å × 170 Å × 170 Å with a grid spacing of 0.375 Å, and CCR-11 docking was performed, keeping FtsZ rigid and CCR-11 as a flexible molecule. The Lamarckian genetic algorithm was employed with the default parameters. Twenty independent docking jobs were conducted, each of 100 runs so that 2000 output conformations were obtained. All the conformations were clustered using a cutoff root-mean-square deviation of 6 Å. The clusters having more than 60 conformations (cutoff number) were selected and analyzed further. An examination of the clusters revealed that few clusters were placed in the same binding regions; therefore, these clusters were further merged. The clusters were then compared on the basis of the cluster size, the binding energies of the conformations, and the decrease in solvent accessible surface area (SASA) of FtsZ due to binding of CCR-11 at that site. A putative binding site for CCR-11 in *B. subtilis* FtsZ was identified. The selected binding site had two clusters in which ligands were placed in two orientations. The lowest-energy conformation of each orientation was selected, and their binding energies were compared. Because the binding energy values were nearly similar, both these conformations were selected (orientations A and B).

Effect of CCR-11 on the Binding of TNP-GTP to FtsZ. TNP-GTP [2′,3′-*O*-(2,4,6-trinitrocyclohexadienylidene)-guanosine 5′-triphosphate], a fluorescent analogue of GTP, was used to check the effect of CCR-11 on the binding of GTP to FtsZ. FtsZ (3 μM) was incubated without and with 3 and 6 μM CCR-11 for 10 min on ice in the presence of buffer A [5 mM $MgCl_2$, 10% glycerol, 200 mM NaCl, and 25 mM Pipes (pH 6.8)]. TNP-GTP (10 μM) was added to each reaction mixture and each mixture further incubated for 1 h on ice. The emission spectra of the reaction milieu were recorded using an excitation wavelength of 410 nm. Fluorescence spectra of only TNP-GTP in buffer A without and with 3 or 6 μM CCR-11 were also recorded. The change in the fluorescence of FtsZ-bound TNP-GTP in the absence and presence of 3 and 6 μM CCR-11 was calculated by subtracting the respective blanks. In addition, the change in TNP-GTP fluorescence was also monitored in the presence of 500 μM GTP.

Determination of the IC_{50} and MIC of CCR-11. An overnight culture of *B. subtilis* cells was diluted to an OD_{600} of 0.05 and was grown in the absence and presence of different concentrations of CCR-11 at 37 °C for 4 h in a 96-well microtiter plate with constant shaking. OD_{600} was measured at the end of 4 h using a Spectramax M2^e multimode reader (Molecular Devices, LLC). The half-maximal inhibitory concentration (IC_{50}) was calculated from the OD_{600} after 4 h for control and CCR-11-treated cells. The experiment was repeated three times. The minimal inhibitory concentration (MIC) of CCR-11 for *B. subtilis* cell proliferation was estimated by an agar dilution assay.[29] The bacterial culture was serially diluted in LB broth, and a total of 1×10^5 cells were spread on each LB agar plate without or with different concentrations (1−7 μM) of CCR-11. The plates were incubated at 37 °C for 12 h, and the number of colonies was counted. The experiment was repeated three times, and each experiment was performed in triplicate. The effect of CCR-11 on the proliferation of *Mycobacterium smegmatis* was tested using the liquid broth assay. Middlebrook 7H9 broth (Himedia) was used to culture *M. smegmatis*. Middlebrook 7H9 medium was prepared according to the manufacturer's protocol. *M. smegmatis* was grown to an OD_{600} of 1. The culture was used to inoculate 5 mL of fresh Middlebrook 7H9 broth without and with different concentrations of CCR-11 and grown at 37 °C in 50 mL conical flasks in an incubator shaker for 18 h. The percentage inhibition of cell proliferation with respect to the control was estimated by measuring OD_{600}. The experiment was repeated three times.

Effect of CCR-11 on the Bacterial Morphology and Z-Ring. The effects of CCR-11 on the Z-ring and nucleoids of *B. subtilis* cells were examined as described previously.[15] *B. subtilis* 168 (OD_{600} ∼ 0.2) cells were incubated in the absence and presence of 2.5 μM CCR-11 for 2 h. The cells were then fixed with 2.5% formaldehyde and 0.04% glutaraldehyde. FtsZ was stained with FtsZ antisera (Bangalore Genei) followed by a Cy3-conjugated goat anti-rabbit secondary antibody (Sigma). Nucleoids were visualized by treating the cells with 2 μg/mL DAPI. Cells were observed using an epifluorescence microscope (Nikon ECLIPSE TE2000-U) with a 100× objective. The images were captured using a Q-imaging camera, and the length of a bacterial cell was measured using Image-Pro Plus (Media Cybernetics, Silver Spring, MD). Alternatively, the FtsZ staining in cells was also visualized using a confocal microscope under a 60× objective. The effect of CCR-11 on the membrane integrity of *B. subtilis* cells was checked using a Live/Dead Baclight bacterial viability kit (Molecular Probes). *B. subtilis* cells were grown in the absence and presence of 2.5 μM CCR-11 for 2 h and then stained with propidium iodide (PI) and SYTO9 as described in the manufacturer's protocol. The cells were put on a glass slide and observed under an epifluorescence microscope (Nikon ECLIPSE TE2000-U) using a 40× objective. The total number of PI-stained cells was counted, and the percentage of PI positive cells was calculated in the control and CCR-11-treated cells. The effect of CCR-11 on the cell membrane was also examined using FM4−64FX (Molecular Probes). The cells were grown in the absence and presence of 2.5 μM CCR-11 for 2 h. Then, the cells were incubated with FM4−64FX (5 μg/mL) for 1 min followed by fixation with 4% formaldehyde for 10 min. The cells were washed thrice with phosphate-buffered saline (pH 7.2) and then stained with DAPI (2 μg/mL). The cells were put on a glass slide and observed using an epifluorescence microscope with a 60× objective.

Effect of CCR-11 on the Proliferation of HeLa Cells. HeLa cells (1×10^5 cells/mL) were seeded in 96-well culture plates. Stocks of the compound were prepared in DMSO. After the cells had been seeded for 24 h, the medium was replaced with fresh medium containing vehicle (0.1% DMSO) or different concentrations of CCR-11. After being incubated for 24 h, cells were fixed with 10% TCA and processed for the sulforhodamine B assay.[30] Data were an average of three independent experiments.

RESULTS

In this study, 151 rhodanine compounds were screened against the growth of *B. subtilis* 168 cells. Of 151 compounds, eight were found to inhibit the growth of *B. subtilis* cells by ≥50% at

2 μM (Table S1 of the Supporting Information). The effects of the eight selected compounds on the morphology of *B. subtilis* were observed under a microscope. Of the eight compounds, three, CCR-4 ((*Z*)-5-{[5-(4-bromophenyl)furan-2-yl]-methylene}-2-thioxothiazolidin-4-one), CCR-11 [(*E*)-2-thio-xo-5-({[3-(trifluoromethyl)phenyl]furan-2-yl}methylene)-thiazolidin-4-one], and CCR-85 ((*Z*)-5-{[5-(2-methoxy-4-nitrophenyl)furan-2-yl]methylene}-2-thioxothiazolidin-4-one) (Figure 1a), were found to cause significant elongation of bacterial cells. While untreated cells had an average cell length of 3.4 ± 0.9 μm, cells treated with CCR-4, CCR-11, and CCR-85 had average cell lengths of 7.4 ± 5, 12 ± 7, and 21 ± 15 μm, respectively (Table S1 of the Supporting Information). Because CCR-4, CCR-11, and CCR-85 significantly increased bacterial cell length, we determined their effects on the GTPase activity of purified FtsZ in vitro.

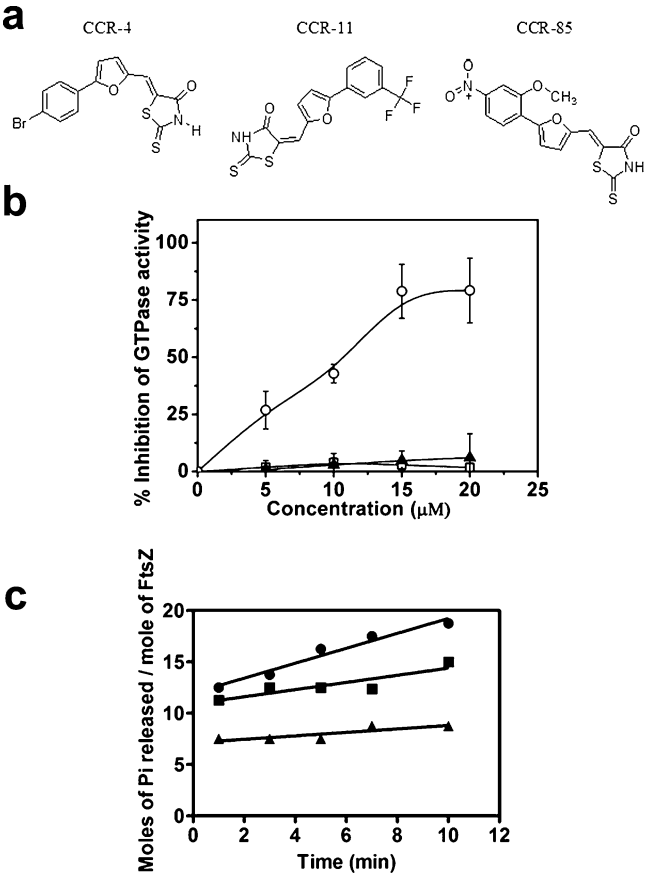

Figure 1. Effects of CCR-4, CCR-11, and CCR-85 on the GTPase activity of FtsZ. (a) Structures of CCR-4 ((*Z*)-5-{[5-(4-bromophenyl)furan-2-yl]methylene}-2-thioxothiazolidin-4-one), CCR-11 [(*E*)-2-thioxo-5-({5-[3-(trifluoromethyl)phenyl]furan-2-yl}-methylene)thiazolidin-4-one], and CCR-85 ((*Z*)-5-{[5-(2-methoxy-4-nitrophenyl)furan-2-yl]methylene}-2-thioxothiazolidin-4-one). (b) Percent inhibition of GTPase activity of FtsZ in the presence of 5, 10, 15, and 20 μM CCR-4 (□), CCR-11 (○), and CCR-85 (▲) with respect to the control. The experiment was performed four times. (c) Rate of GTP hydrolysis of FtsZ monitored in the absence (●) and presence of 5 (■) and 10 μM CCR-11 (▲). The experiment was performed three times.

CCR-11 Inhibited the GTPase Activity of FtsZ. The effect of different concentrations of CCR-4, CCR-11, and CCR-85 on the GTPase activity of *Bacillus* FtsZ was checked. CCR-4 and CCR-85 did not significantly affect the GTPase activity of FtsZ (Figure 1b). However, CCR-11 was found to inhibit the GTPase activity of FtsZ in a concentration-dependent manner (Figure 1b). For example, 5 and 20 μM CCR-11 reduced the amount of inorganic phosphate released per mole of FtsZ by 27 ± 8 and 79 ± 14%, respectively, as compared to the control (Figure 1b). The IC_{50} of CCR-11 for the GTPase activity of FtsZ was calculated to be 10.6 ± 0.5 μM. Further, CCR-11 was also found to decrease the rate of GTP hydrolysis of FtsZ. The rates of GTP hydrolysis in the absence and presence of 5 and 10 μM CCR-11 were estimated to be 0.73 ± 0.08, 0.35 ± 0.1, and 0.17 ± 0.06 mol of P_i (mol of FtsZ)$^{-1}$ min^{-1}, respectively (Figure 1c). The GTPase activity of FtsZ is known to influence the assembly dynamics of FtsZ, and it is considered to be crucial for the function of FtsZ. Because CCR-4 and CCR-85 had no effect on the GTPase activity of FtsZ, we opted to study the effect of CCR-11 on the assembly of FtsZ and to elucidate its effects on Z-ring formation and bacterial cell division.

CCR-11 Inhibited the Assembly of FtsZ Protofilaments. The effect of CCR-11 on the assembly kinetics of FtsZ was monitored using 90° light scattering. CCR-11 was found to inhibit the rate and extent of FtsZ assembly in a concentration-dependent manner (Figure 2a). The extent of FtsZ assembly at 5 min was inhibited by 18 ± 8, 37 ± 13, and 71 ± 14% in the presence of 5, 10, and 20 μM CCR-11, respectively, as compared to control (Figure 2a). The morphology of FtsZ polymers in the absence and presence of CCR-11 was examined using electron microscopy (Figure 2b). Under the conditions used for assembly, FtsZ formed thick filaments and bundles in the absence of the compound. CCR-11 (5 μM) strongly reduced the number of FtsZ polymers per observation field and also inhibited the bundling of FtsZ protofilaments (Figure 2b). CCR-11 (20 μM) inhibited the assembly of FtsZ and also induced the aggregation of short FtsZ filaments (Figure 2b). Using light scattering and electron microscopy, we

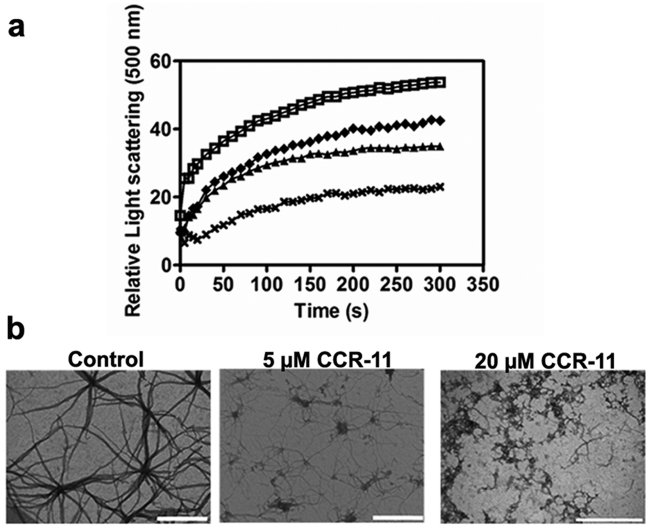

Figure 2. Effects of CCR-11 on the assembly of FtsZ. (a) FtsZ (8 μM) was incubated without (□) or with 5 (◆), 10 (▲), and 20 μM CCR-11 (×) for 10 min on ice and polymerized at 37 °C. The assembly of FtsZ was monitored using 90° light scattering at 500 nm. One of four independent experiments is shown. The inhibition data are averages of four experiments. (b) The morphology of FtsZ polymers was examined in the presence of different concentrations of CCR-11 using electron microscopy. The scale bar is 500 nm.

dx.doi.org/10.1021/bi201813u | *Biochemistry* 2012, 51, 5434−5442

found that FtsZ with and without the His tag showed similar assembly characteristics (Figure S1 of the Supporting Information). Further, CCR-11 was found to potently inhibit the assembly of FtsZ without the His tag (Figure S1 of the Supporting Information). Because CCR-11 affected the assembly of FtsZ without and with the His tag in a similar manner, we used FtsZ with the His tag for the rest of the experiments.

Characterization of the Binding of CCR-11 to FtsZ. Y273W-FtsZ displayed a typical emission spectrum, and CCR-11 quenched the tryptophan fluorescence of Y273W-FtsZ in a concentration-dependent fashion, indicating that CCR-11 interacts with FtsZ (Figure 3a). A dissociation constant of 1.5 ± 0.3 μM for the interaction of CCR-11 and Y273W-FtsZ was determined using the fluorescence data (Figure 3b).

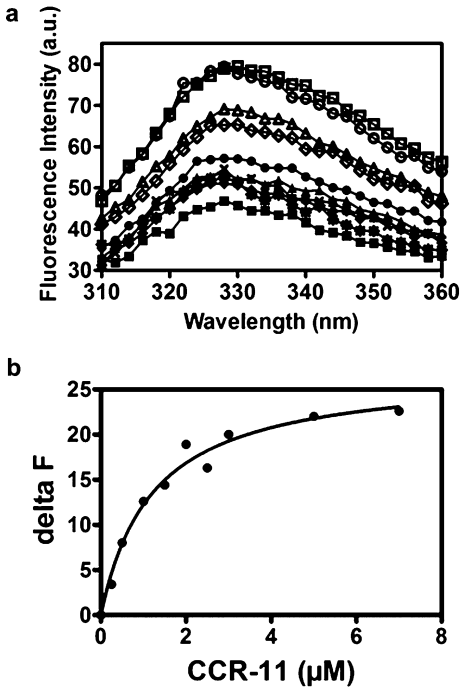

Figure 3. CCR-11 binds to FtsZ in vitro. Y273W-FtsZ (0.5 μM) was incubated without (□) or with different concentrations of CCR-11. (a) There was a decrease in the tryptophan fluorescence in the presence of 0.25 (○), 0.5 (△), 1.0 (◇), 1.5 (●), 2.0 (▲), 2.5 (◆), 3.0 (×), 5.0 (∗), and 7.0 μM CCR-11 (■). (b) The change in the tryptophan fluorescence intensity (at 330 nm) of Y273W-FtsZ was plotted vs the concentration of CCR-11. The experiment was performed four times.

Further, docking analysis predicted that CCR-11 binds to FtsZ in a cavity adjacent to the T7 loop (Figure 4). The amino acid residues within the 4 Å region of CCR-11 include Asp 199, Thr 203, Pro 204, Gly 205, Leu 206, Ile 207, Asn 208, Leu 270, Ser 271, Leu 272, Val 275, Ser 296, Val 297, and Ile 298. The analysis suggested that CCR-11 might bind to FtsZ at this site in two orientations, one with trifluoromethylphenyl side chain toward the cavity (orientation A) (Figure 4a, i and ii) and the other having the thiazolidine ring facing the binding pocket (orientation B) (Figure 4b, i and ii). The estimated binding energies for orientations A and B were −7.65 and −7.00 kcal/mol, respectively, indicating that CCR-11 may bind to FtsZ in both conformations as the energy difference between these conformations is not too large. In orientation A, short-range halogen−oxygen interactions[31] were observed between CCR-11 and the surrounding amino acid residues. For example, two of the fluorine atoms of the trifluoromethylphenyl side chain of CCR-11 were interacting with the main chain carbonyl oxygen and side chain hydroxyl oxygen of Thr 203. In addition, many of the binding site residues like Gly 205, Ile 207, Leu 272, Val 275, and Ileu 298 may be involved in hydrophobic interactions with CCR-11 (Figure 4a, iii). In orientation B the distances from the NH of the thiazolidine ring of CCR-11 to the hydroxyl oxygen of Thr 203 and the main chain carbonyl oxygen of Asp 199 were measured to be 3.0 and 3.2 Å, respectively, indicating the possibility of hydrogen bonds between the two pairs. Hydrophobic interactions were also observed with amino acids like Ile 298, Leu 206, and Val 297 in this conformation (Figure 4b, iii).

CCR-11 Did Not Inhibit the Binding of TNP-GTP to FtsZ. TNP-GTP has been used to monitor the binding of GTP to FtsZ.[16,32] The fluorescence intensity of TNP-GTP was found to increase by 48 ± 7% in the presence of FtsZ, indicating the binding of TNP-GTP to FtsZ. GTP (500 μM) reduced the fluorescence enhancement of TNP-GTP in the presence of FtsZ by 72 ± 8%, suggesting that GTP and TNP-GTP compete for the same binding site on FtsZ (Figure S2 of the Supporting Information). CCR-11 (3 or 6 μM) had no significant effect on the fluorescence intensity of TNP-GTP bound to FtsZ. The fluorescence intensity of TNP-GTP-bound FtsZ was reduced by 1.4 ± 2.5 and 7.4 ± 10.6% in the presence of 3 and 6 μM CCR-11, respectively (Figure S2 of the Supporting Information). TNP-GTP has been found to bind to FtsZ with a dissociation constant of 10 ± 2.7 μM (data not shown). The results suggested that CCR-11 does not inhibit the binding of GTP to FtsZ and that CCR-11 binds at a site distinct from the GTP binding site on FtsZ.

CCR-11 Inhibited the Proliferation of *B. subtilis* and *M. smegmatis* Cells. CCR-11 was found to inhibit the growth of *B. subtilis* cells in a concentration-dependent manner with an IC_{50} of 1.2 ± 0.2 μM (Figure 5). To estimate MIC, 1×10^5 cells were plated on agar plates without or with different concentrations of CCR-11. The number of colony-forming units per milliliter in the presence of different concentrations of CCR-11 suggested that CCR-11 strongly inhibited the proliferation of *B. subtilis* cells with an MIC of 3 μM (Table S2 of the Supporting Information). Further, CCR-11 also significantly inhibited the proliferation of *M. smegmatis* cells. In the presence of 1 and 4 μM CCR-11, the growth of *M. smegmatis* cells after 15 h was inhibited by 72 ± 5 and 98 ± 2%, respectively, with respect to the control.

CCR-11 Inhibited Z-Ring Formation in *B. subtilis* Cells. The effects of CCR-11 on Z-ring formation and nucleoid segregation in *B. subtilis* cells were examined by fluorescence microscopy. Consistent with the previous reports,[14−16] 63% of the control cells had a distinct Z-ring at the cell center (Figure 6a). However, only ∼4% of the cells showed the presence of the Z-ring in the presence of 2.5 μM CCR-11. The CCR-11-treated cells were elongated compared to the control cells. The numbers of nucleoids per micrometer of cell length in control cells and cells treated with 2.5 μM CCR-11 were determined to be 0.55 ± 0.15 and 0.51 ± 0.24, respectively, suggesting that CCR-11 did not affect nucleoid segregation. However, CCR-11 treatment strongly perturbed Z-ring formation in *B. subtilis* cells (Figure 6a,b). The fluorescence signal of FtsZ in cells treated with CCR-11 was delocalized and found to be present as helices throughout the cell (Figure 6a,b). FtsZ in the treated

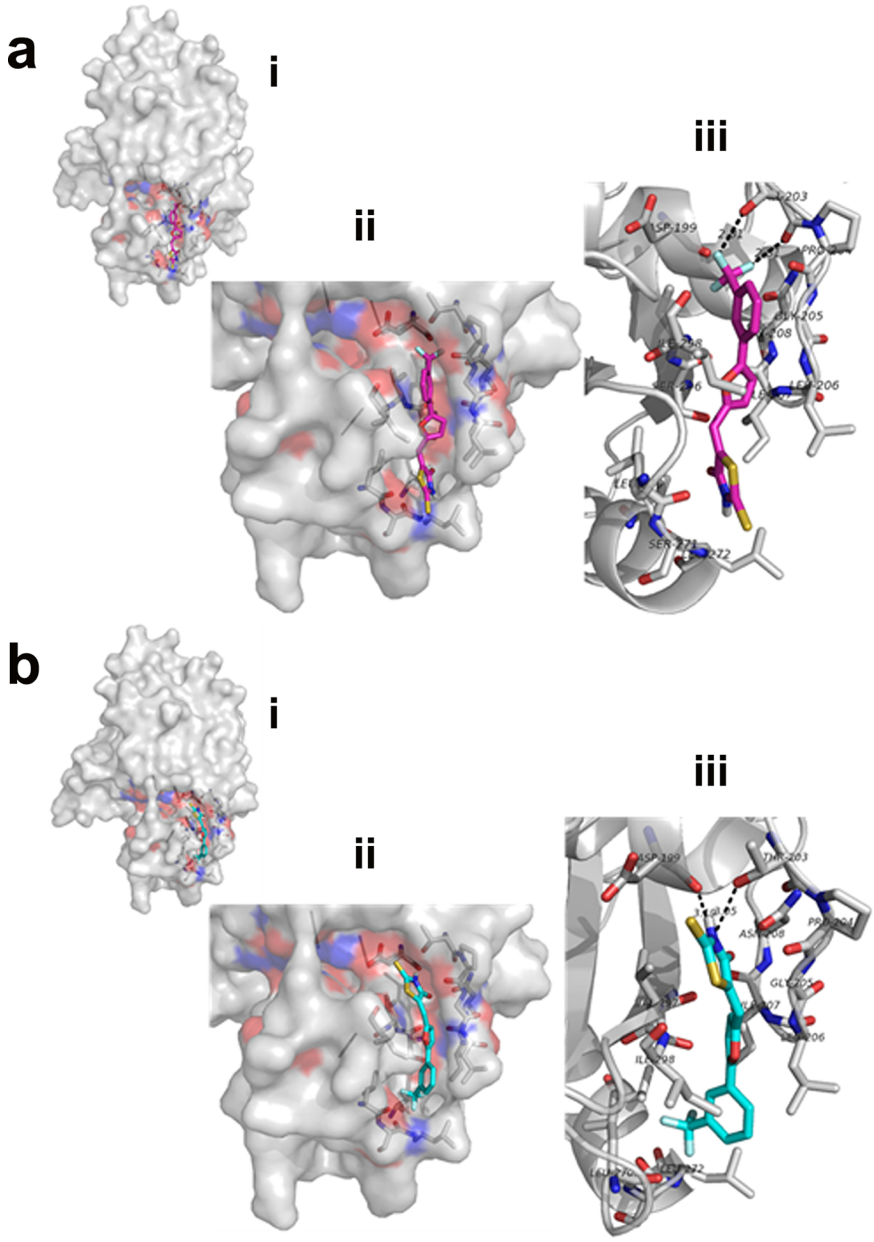

Figure 4. Docking analysis of the binding of CCR-11 and FtsZ. (a) Binding of CCR-11 in *B. subtilis* FtsZ in orientation A. (b) Binding of CCR-11 in *B. subtilis* FtsZ in orientation B. In both panels a and b, different subpanels show (i) the location of CCR-11 in the FtsZ monomer, (ii) a close-up image of the CCR-11 binding cavity, and (iii) interactions of CCR-11 with binding site residues. This figure was drawn using PyMol.[36] CCR-11 is colored magenta and cyan in orientations A and B, respectively, and FtsZ is colored gray.

cells was also found to be localized in the form of spots on the membrane. The number of Z-rings per unit cell length in the control cells was determined to be 0.14 ± 0.09 μm^{-1}. In the presence of 1 μM CCR-11, the frequency of occurrence of the Z-ring per micrometer of cell length was strongly reduced and no distinct Z-ring was visible in the cells treated with 2.5 μM CCR-11. The results together suggested that CCR-11 inhibits proliferation of bacterial cells by inhibiting FtsZ assembly and disrupting the Z-rings in the cells.

CCR-11 Did Not Perturb the Integrity of the Cell Membrane. To check whether CCR-11 might damage the cell membrane, the cells were grown in the absence and presence of CCR-11 (2.5 μM) for 2 h and stained with propidium iodide and SYTO9 using the Live/Dead Baclight bacterial viability kit. The percentages of propidium iodide-stained cells in control cells and cells treated with 2.5 μM CCR-11 were found to be 4.9 ± 0.9 and 5.3 ± 1.6%, respectively (Figure S3 of the Supporting Information). The result indicated that CCR-11 did not detectably perturb the membrane integrity of *B. subtilis* cells. Further, *B. subtilis* cells were also stained with FM4–64FX, a lipophilic styryl dye, and DAPI, a nucleic acid stain. The control cells showed a clear membrane and complete septa at the cell center. In the cells treated with CCR-11 (2.5 μM), a majority of these septa were irregular and mostly incomplete; however, a few septa appeared to be touching both sides of the membrane. Many of the incomplete septa were found to localize on the nucleoids rather than between the nucleoids (Figure 6c). Because nucleoid segregation was found to be unaffected by CCR-11, the mislocalization of FtsZ in CCR-11-

dx.doi.org/10.1021/bi201813u | *Biochemistry* 2012, 51, 5434–5442

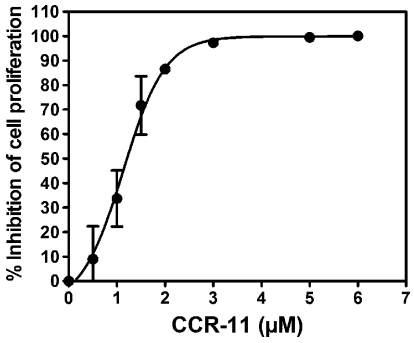

Figure 5. Effects of CCR-11 on the proliferation of *B. subtilis* cells. *B. subtilis* cells were grown in the absence and presence of different concentrations of CCR-11 for 4 h at 37 °C, and the IC_{50} was calculated from a dose-dependent growth curve. The experiment was performed three times.

treated cells may be responsible for the formation of incomplete septa over the nucleoids.

Effects of CCR-11 on the Proliferation of HeLa Cells. FtsZ is a homologue of eukaryotic cytoskeletal protein tubulin. Therefore, we checked whether CCR-11 could inhibit the proliferation of mammalian cells. HeLa cells were grown in the absence and presence of different concentrations of CCR-11. CCR-11 did not strongly inhibit the proliferation of HeLa cells. For example, 9 μM CCR-11 (~8 × IC_{50} of *B. subtilis* cell proliferation) was found to inhibit HeLa cell proliferation in culture by 13.5 ± 7.4%, and 50% inhibition of HeLa cell proliferation occurred in the presence of 18.1 ± 0.2 μM compound.

DISCUSSION

Because of the widespread use of commonly used antibiotics, several pathogenic strains of bacteria have developed resistance against them. This emphasizes the need for identification of novel antibacterial drugs as well as drug targets. FtsZ, an essential cell division protein, is emerging as an important and exploitable drug target. In view of this, several groups have put efforts into identifying agents that inhibit bacterial cell division by targeting FtsZ.[14−21] For example, PC190723, one of the potent FtsZ targeting synthetic compounds, was found to inhibit the growth of *Staphylococcus aureus* both in vitro and in animal models.[18] Different FtsZ-targeted agents led to the inhibition of bacterial cell proliferation by different mechanisms, further strengthening the idea that the perturbation of FtsZ assembly dynamics can be an important strategy for developing antibacterial drugs. OTBA, PC190723, 8j, and a few zantrins have been reported to inhibit bacterial cell division by promoting FtsZ assembly and stabilizing FtsZ protofilaments.[15,17,18,21]

In this study, we identified an FtsZ-targeted antibacterial agent, CCR-11. Similar to the action of several FtsZ-targeted agents such as totarol, sanguinarine, PC190723, 8j, and OTBA,[14−16,18,21] CCR-11 was found to cause elongation of *B. subtilis* cells and to perturb the formation of the Z-ring without affecting nucleoid segregation. To further probe whether CCR-11 perturbs nucleoid segregation in elongated

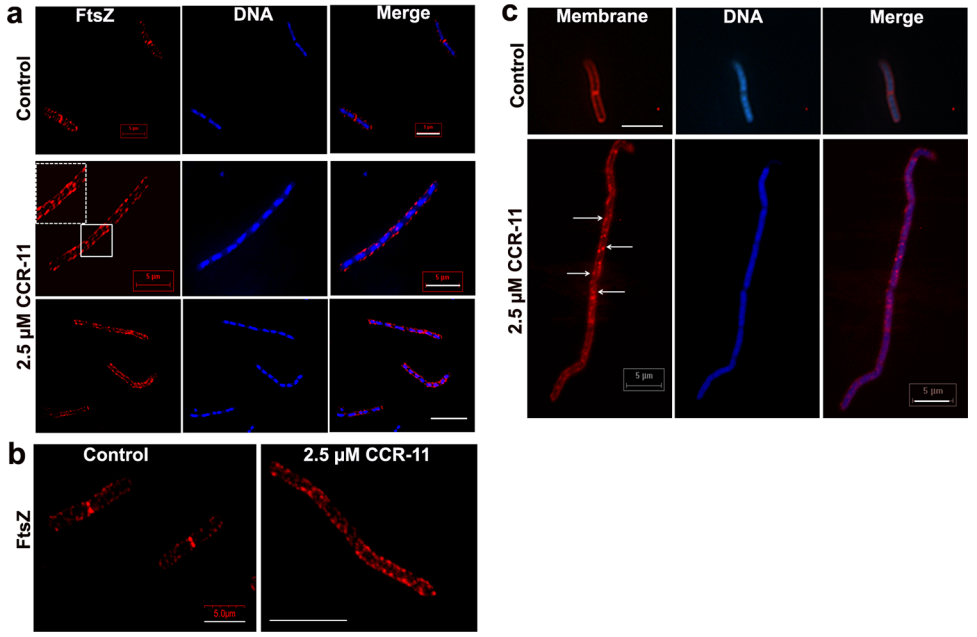

Figure 6. Effects of CCR-11 on the Z-ring, nucleoids, and membrane in *B. subtilis* cells. (a) Effects of CCR-11 on the Z-ring and nucleoids. *B. subtilis* cells were grown in the absence or presence of 2.5 μM CCR-11 for 2 h. FtsZ was stained using FtsZ antisera followed by a Cy3-conjugated goat anti-rabbit secondary antibody, and nucleoids were stained with DAPI and cells observed under an epifluorescence microscope using a 100× objective. We scored 500 cells for each experimental condition. The inset in CCR-11-treated cells shows a close-up of the area marked with a solid square. The scale bar is 5 μm. (b) Confocal images of *B. subtilis* cells stained for FtsZ in the absence and presence of CCR-11 observed under a 60× objective. The images are magnified to show the details of FtsZ inside the cells. In control cells, FtsZ was present as the Z-ring at the midcell. The cells treated with CCR-11 (2.5 μM) showed no Z-ring at the midcell; instead, FtsZ was present as helices and spots throughout the cell length. The scale bars are 5 and 10 μm in control cells and cells treated with CCR-11, respectively. (c) Effects of CCR-11 on the membrane of *B. subtilis* cells. *B. subtilis* cells were grown in the absence or presence of 2.5 μM CCR-11 for 2 h at 37 °C. The cell membranes were then stained using FM4−64FX, and DNA was stained using DAPI. The cells were observed under an epifluorescence microscope using a 60× objective. The arrows indicate the presence of incomplete septa in the CCR-11-treated cells. The scale bar is 5 μm.

dx.doi.org/10.1021/bi201813u | *Biochemistry* 2012, 51, 5434−5442

cells, we carefully examined nucleoid segregation in the highly elongated (cell length of ≥24 nm) cells (Figure S4 of the Supporting Information). The analysis indicated that CCR-11 did not noticeably influence nucleoid segregation. However, it is difficult to completely rule out the possibility that a small fraction of the highly filamentous cells may have a defect in nucleoid segregation.

In CCR-11-treated cells, FtsZ staining was delocalized and present along the length of the cells as helices or spots on the membrane (Figure 6b). The spots may be due to the accumulation of FtsZ at the turn of the helical filaments or random accumulation of mislocalized FtsZ at the membrane. Further, the membrane staining of CCR-11-treated cells also revealed the presence of incomplete and irregular septa along the cell length. The cells treated with CCR-11 were elongated and could not undergo division, indicating that the septa formed are nonfunctional. The perturbation of FtsZ assembly in the CCR-11-treated cells might produce these defective septa.

Several microtubule targeting agents are known to inhibit mitosis by suppressing microtubule dynamics without visibly depolymerizing cellular microtubules.[33,34] These compounds in their low inhibitory concentration range perturb the dynamics of spindle microtubules and cause the formation of nonfunctional aberrant spindles, leading to a mitotic block and inhibition of cell division.[33,34] Similar to the action of microtubule-targeted agents, CCR-11 may inhibit bacterial division by perturbing the assembly dynamics of FtsZ in the Z-ring without completely destroying them.

FtsZ-targeted agents appear to inhibit the bacterial proliferation either by stabilizing and enhancing FtsZ assembly like PC190723, 8j, zantrins, and OTBA or by inhibiting FtsZ assembly like totarol and sanguinarine. CCR-11 was found to perturb bacterial cytokinesis by inhibiting the assembly of FtsZ. Like PC190723, 8j, zantrins, and OTBA, CCR-11 was also found to inhibit the GTPase activity of FtsZ. Using TNP-GTP, a fluorescent analogue of GTP, we found that CCR-11 had no effect on the binding of TNP-GTP to FtsZ (Figure S2 of the Supporting Information), suggesting that CCR-11 does not affect the binding of GTP to FtsZ. The docking analysis indicated that CCR-11, like PC190723, binds to FtsZ at a site distinct from the GTP binding site. However, the residues that constitute the CCR-11 binding pocket are part of the T7 loop of FtsZ. The interaction of the T7 loop with the GTP binding motif is essential for FtsZ polymerization.[35] The binding of CCR-11 might perturb the polymerization of FtsZ directly by inhibiting the interaction of the T7 loop of an FtsZ monomer with the GTP binding site of another FtsZ monomer, thereby reducing GTPase activity and inhibiting the assembly of FtsZ.

CCR-11 bound to FtsZ with a dissociation constant of 1.5 ± 0.3 μM, suggesting that it binds to FtsZ with a higher affinity than many other FtsZ inhibitors.[14−16] The docking analysis revealed that CCR-11 binds to *Bacillus* FtsZ at a site in two possible orientations (Figure 4). The theoretical K_d values of binding of CCR-11 to FtsZ in the two orientations, A and B, were estimated to be 2.5 and 7.4 μM, respectively. The value of the experimentally determined K_d (1.5 μM) was found to be similar to the theoretically estimated K_d for the two orientations (2.5 and 7.4 μM for orientations A and B, respectively), further corroborating the docking analysis.

The assembly dynamics of cytoskeletal polymers plays a crucial role in cell division. Several compounds that either promote or inhibit the assembly of tubulin, a eukaryotic homologue of FtsZ, are in clinical use as anticancer drugs. Similarly, small molecules such as CCR-11, OTBA, and PC190723 that inhibit bacterial proliferation either by inhibiting or by enhancing FtsZ polymerization may also have the potential to be developed as prospective antibacterial drugs.

■ ASSOCIATED CONTENT

Supporting Information

Table S1 lists eight compounds that were found to inhibit the proliferation of *B. subtilis* 168 cells by ≥50% at 2 μM. Table S2 lists the decreases in values of colony-forming units per milliliter in the presence of different concentrations of CCR-11. Figure S1 shows that the presence of the His tag did not visibly influence the assembly kinetics or the bundling of FtsZ. Additionally, it also shows that CCR-11 potently inhibits the assembly of FtsZ without the His tag. Figure S2 shows the effect of CCR-11 on the binding of TNP-GTP to FtsZ. Figure S3 shows the effect of CCR-11 on the membrane integrity and cell viability of *B. subtilis*. The results suggest that CCR-11 inhibits bacterial cytokinesis without perturbing the membrane integrity of *B. subtilis* cells. Figure S4 shows the effect of CCR-11 on the nucleoid segregation in filamentous cells. CCR-11 did not detectably perturb the nucleoid segregation in *B. subtilis* cells. This material is available free of charge via the Internet at http://pubs.acs.org.

■ AUTHOR INFORMATION

Corresponding Author

*D.P.: Indian Institute of Technology Bombay, Mumbai 400076, India; phone, +91-22-25767838; fax, +91-22-25723480; e-mail, panda@iitb.ac.in. A.S.: Molecular Biophysics Unit, Indian Institute of Science, Bangalore 560012, India; phone, +91-80-22932389; e-mail, surolia@mbu.iisc.ernet.in.

Funding

The work is partly funded by a grant from the Department of Science and Technology, Government of India, to D.P. and partly by a J. C. Bose fellowship to A.S. from the Department of Science and Technology, Government of India.

Notes

The authors declare no competing financial interest.

■ ACKNOWLEDGMENTS

We thank Jayant Asthana for his help with checking the effect of CCR-11 on HeLa cell proliferation and electron microscopy studies.

■ ABBREVIATIONS

CCR-11, (*E*)-2-thioxo-5-({[3-(trifluoromethyl)phenyl]furan-2-yl}methylene)thiazolidin-4-one; IC_{50}, half-maximal inhibitory concentration; Pipes, piperazine-1,4-bis(2-ethanesulfonic acid); IPTG, isopropyl β-D-1-thiogalactopyranoside; TNP-GTP, 2′,3′-*O*-(2,4,6-trinitrocyclohexadienylidene)guanosine 5′-triphosphate.

■ REFERENCES

(1) Lutkenhaus, J. F., Wolf-Watz, H., and Donachie, W. D. (1980) Organization of genes in the *ftsA-envA* region of the *Escherichia coli* genetic map and identification of a new *fts* locus (*ftsZ*). *J. Bacteriol. 142*, 615−620.

(2) Bi, E., and Lutkenhaus, J. (1992) Isolation and characterization of *ftsZ* alleles that affect septal morphology. *J. Bacteriol. 174*, 5414−5423.

(3) Adams, D. W., and Errington, J. (2009) Bacterial cell division: Assembly, maintenance and disassembly of the Z ring. *Nat. Rev. Microbiol. 7*, 642−653.
(4) Anderson, D. E., Gueiros-Filho, F. J., and Erickson, H. P. (2004) Assembly dynamics of FtsZ rings in *Bacillus subtilis* and *Escherichia coli* and effects of FtsZ-regulating proteins. *J. Bacteriol. 186*, 5775−5781.
(5) Stricker, J., Maddox, P., Salmon, E. D., and Erickson, H. P. (2002) Rapid assembly dynamics of the *Escherichia coli* FtsZ-ring demonstrated by fluorescence recovery after photobleaching. *Proc. Natl. Acad. Sci. U.S.A. 99*, 3171−3175.
(6) Addinall, S. G., and Lutkenhaus, J. (1996) FtsA is localized to the septum in an FtsZ-dependent manner. *J. Bacteriol. 178*, 7167−7172.
(7) Dai, K., Mukherjee, A., Xu, Y., and Lutkenhaus, J. (1994) Mutations in ftsZ that confer resistance to SulA affect the interaction of FtsZ with GTP. *J. Bacteriol. 176*, 130−136.
(8) Kapoor, S., and Panda, D. (2009) Targeting FtsZ for antibacterial therapy: A promising avenue. *Expert Opin. Ther. Targets 13*, 1037−1051.
(9) Jaiswal, R., Patel, R. Y., Asthana, J., Jindal, B., Balaji, P. V., and Panda, D. (2010) E93R substitution of *Escherichia coli* FtsZ induces bundling of protofilaments, reduces GTPase activity, and impairs bacterial cytokinesis. *J. Biol. Chem. 285*, 31796−31805.
(10) Lu, C., Stricker, J., and Erickson, H. P. (2001) Site-specific mutations of FtsZ: Effects on GTPase and in vitro assembly. *BMC Microbiol. 1*, 1−7.
(11) Singh, P., and Panda, D. (2010) FtsZ inhibition: A promising approach for antistaphylococcal therapy. *Drug News Perspect. 23*, 295−304.
(12) Vollmer, W. (2006) The prokaryotic cytoskeleton: A putative target for inhibitors and antibiotics? *Appl. Microbiol. Biotechnol. 73*, 37−47.
(13) Schaffner-Barbero, C., Martín-Fontecha, M., Chacón, P., and Andreu, J. M. (2012) Targeting the Assembly of Bacterial Cell Division Protein FtsZ with Small Molecules. *ACS Chem. Biol. 7*, 267−277.
(14) Beuria, T. K., Santra, M. K., and Panda, D. (2005) Sanguinarine blocks cytokinesis in bacteria by inhibiting FtsZ assembly and bundling. *Biochemistry 44*, 16584−16593.
(15) Beuria, T. K., Singh, P., Surolia, A., and Panda, D. (2009) Promoting assembly and bundling of FtsZ as a strategy to inhibit bacterial cell division: A new approach for developing novel antibacterial drugs. *Biochem. J. 423*, 61−69.
(16) Jaiswal, R., Beuria, T. K., Mohan, R., Mahajan, S. K., and Panda, D. (2007) Totarol inhibits bacterial cytokinesis by perturbing the assembly dynamics of FtsZ. *Biochemistry 46*, 4211−4220.
(17) Margalit, D. N., Romberg, L., Mets, R. B., Hebert, A. M., Mitchison, T. J., Kirschner, M. W., and Raychaudhuri, D. (2004) Targeting cell division: Small-molecule inhibitors of FtsZ GTPase perturb cytokinetic ring assembly and induce bacterial lethality. *Proc. Natl. Acad. Sci. U.S.A. 101*, 11821−11826.
(18) Haydon, D. J., Stokes, N. R., Ure, R., Galbraith, G., Bennett, J. M., Brown, D. R., Baker, P. J., Barynin, V. V., Rice, D. W., Sedelnikova, S. E., Heal, J. R., Sheridan, J. M., Aiwale, S. T., Chauhan, P. K., Srivastava, A., Taneja, A., Collins, I., Errington, J., and Czaplewski, L. G. (2008) An inhibitor of FtsZ with potent and selective anti-staphylococcal activity. *Science 321*, 1673−1675.
(19) Ito, H., Ura, A., Oyamada, Y., Tanitame, A., Yoshida, H., Yamada, S., Wachi, M., and Yamagishi, J. (2006) A 4-aminofurazan derivative-A189-inhibits assembly of bacterial cell division protein FtsZ in vitro and in vivo. *Microbiol. Immunol. 50*, 759−764.
(20) Reynolds, R. C., Srivastava, S., Ross, L. J., Suling, W. J., and White, E. L. (2004) A new 2-carbamoyl pteridine that inhibits mycobacterial FtsZ. *Bioorg. Med. Chem. Lett. 14*, 3161−3164.
(21) Adams, D. W., Wu, L. J., Czaplewski, L. G., and Errington, J. (2011) Multiple effects of benzamide antibiotics on FtsZ function. *Mol. Microbiol. 80*, 68−84.
(22) Tomasić, T., and Masic, L. P. (2009) Rhodanine as a privileged scaffold in drug discovery. *Curr. Med. Chem. 16*, 1596−1629.
(23) Bradford, M. M. (1976) A rapid and sensitive method for the quantitation of microgram quantities of protein utilizing the principle of protein-dye binding. *Anal. Biochem. 72*, 248−254.
(24) Lu, C., Stricker, J., and Erickson, H. P. (1998) FtsZ from *Escherichia coli*, *Azotobacter vinelandii*, and *Thermotoga maritima*: Quantitation, GTP hydrolysis, and assembly. *Cell Motil. Cytoskeleton 40*, 71−86.
(25) Geladopoulos, T. P., Sotiroudis, T. G., and Evangelopoulos, A. E. (1991) A malachite green colorimetric assay for protein phosphatase activity. *Anal. Biochem. 192*, 112−116.
(26) Morris, G. M., Goodsell, D. S., Halliday, R. S., Huey, R., Hart, W. E., Belew, R. K., and Olson, A. J. (1998) Automated Docking Using a Lamarckian Genetic Algorithm and Empirical Binding Free Energy Function. *J. Comput. Chem. 19*, 1639−1662.
(27) Berman, H. M., Westbrook, J., Feng, Z., Gilliland, G., Bhat, T. N., Weissig, H., Shindyalov, I. N., and Bourne, P. E. (2000) The Protein Data Bank. *Nucleic Acids Res. 28*, 235−242.
(28) Schüttelkopf, A. W., and van Aalten, D. M. (2004) PRODRG: A tool for high-throughput crystallography of protein-ligand complexes. *Acta Crystallogr. D60*, 1355−1363.
(29) Wiegand, I., Hilpert, K., and Hancock, R. E. (2008) Agar and broth dilution methods to determine the minimal inhibitory concentration (MIC) of antimicrobial substances. *Nat. Protoc. 3*, 163−175.
(30) Skehan, P., Storeng, R., Scudiero, D., Monks, A., McMahon, J., Vistica, D., Warren, J. T., Bokesch, H., Kenney, S., and Boyd, M. R. (1990) New colorimetric cytotoxicity assay for anticancer-drug screening. *J. Natl. Cancer Inst. 82*, 1107−1112.
(31) Auffinger, P., Hays, F. A., Westhof, E., and Ho, P. S. (2004) Halogen bonds in biological molecules. *Proc. Natl. Acad. Sci. U.S.A. 101*, 16789−16794.
(32) Mukherjee, A., Santra, M. K., Beuria, T. K., and Panda, D. (2005) A natural osmolyte trimethylamine N-oxide promotes assembly and bundling of the bacterial cell division protein, FtsZ and counteracts the denaturing effects of urea. *FEBS J. 272*, 2760−2772.
(33) Jordan, M. A., and Wilson, L. (2004) Microtubules as a target for anticancer drugs. *Nat. Rev. Cancer 4*, 253−265.
(34) Dumontet, C., and Jordan, M. A. (2010) Microtubule-binding agents: A dynamic field of cancer therapeutics. *Nat. Rev. Drug Discovery 9*, 790−803.
(35) Scheffers, D. J., de Wit, J. G., den Blaauwen, T., and Driessen, A. J. (2002) GTP hydrolysis of cell division protein FtsZ: Evidence that the active site is formed by the association of monomers. *Biochemistry 41*, 521−529.
(36) DeLano, W. L. (2002) *The PyMOL Molecular Genetics Graphics System*, DeLano Scientific LLC, San Carlos, CA.